BUILDING CLASSIFICATION USING AIRBORNE LIDAR DATA WITH SATELLITE SAR DATA

Tatsuya Yamamoto, Masafumi Nakagawa
Shibaura Institute of Technology, 3-7-5, Toyosu, Koto-ku, Tokyo, 135-8548, Japan
Email: h10082@shibaura-it.ac.jp

KEY WORDS: Satellite SAR, Airborne LiDAR, Urban mapping, Building classification

ABSTRACT: In general, airborne photogrammetry and LiDAR measurements are applied to geometrical data acquisition for automated map generation and revision. However, attribute data acquisition and classification depend on manual editing works including ground surveys. On the other hand, SAR data have a possibility to automate the attribute data acquisition and classification. Thus, we focus on an integration of LiDAR and SAR data to achieve a frequent map update with attribute data acquisition. In this study, we use airborne LiDAR and satellite SAR data to classify buildings. Firstly, we generate a digital surface model (DSM) from point cloud acquired with airborne LiDAR. Secondary, the DSM is registered with a normalized radar cross section (NRCS) image calculated from SAR data. Thirdly, buildings are extracted from the DSM. Finally, the buildings are classified into several clusters in the DSM. We clarified that a combination of airborne LiDAR and satellite SAR data can extract and classify buildings in urban area.

1. INTRODUCTION

A frequent map revision is required in GIS applications, such as disaster prevention and urban planning. In general, airborne photogrammetry and LiDAR measurements are applied to geometrical data acquisition for automated map generation and revision. In the airborne photogrammetry, a geometrical modeling and object classification can be automated using color images. Stereo matching is an essential technique to reconstruct 3D model from images. Recently, structure from motion (SfM) is proposed to generate 3D mesh model from random images (Uchiyama, 2014). Although, object classification methods are automated using height data estimated with stereo matching and SfM, it is difficult to recognize construction materials, such as woods and concrete. The construction materials are significant attribute data in building modeling and mapping. Therefore, ground survey and manual editing works are required in attribute data classification.
In the LiDAR measurements, modeling and object classification are also automated by a segmentation of point cloud data (Sithole, 2003). The intensity data also assist the object classification (Antonarakis, 2008). Moreover, data fusion approaches are proposed using aerial images and LiDAR data. These approaches focus on modeling accuracy improvement and processing time improvement (Uemura, 2011). However, these approaches classify geometrical attributes.
On the other hand, although geometrical data extraction is difficult, SAR data have a possibility to automate the attribute data acquisition and classification. The SAR data represent microwave reflections on various surfaces of ground and buildings. There are many researches related to monitoring activities of disaster, vegetation, and urban. Moreover, we have an opportunity to acquire higher resolution data in urban areas with new sensors, such as ALOS2 PALSAR2 (Japan Aerospace Exploration Agency, 2014). Therefore, in this study, we focus on an integration of airborne LiDAR data and satellite SAR data for building extraction and classification.

2. METHODOLOGY

Our process is shown in Figure 1. Firstly, we generate DSM and reflection intensity orthoimage from LiDAR point cloud data. Secondary, these data are registered using corresponded points taken from each datum. Thirdly, buildings are extracted from the DSM. Finally, buildings are classified with normalized radar cross section (NRCS) calculated using SAR data.

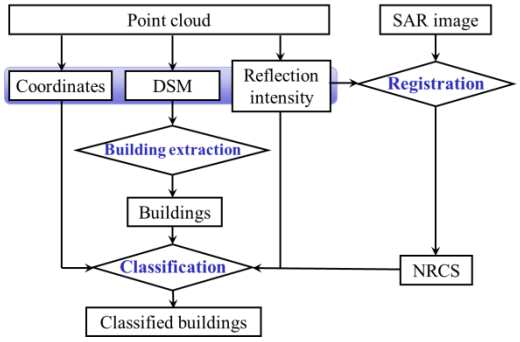

Figure 1. Our process flow

2.1 Registration of LiDAR and SAR data

In a registration between SAR and LiDAR data, corresponded points are required to be extracted from each datum. Although SAR data and LiDAR data have different indices, we can recognize road intersections, rivers, and bridges as feature points in manual.
Before a feature extraction procedure, two types of orthoimages are prepared as follows. Firstly, digital number (DN) of SAR image is converted into an orthoimage of NRCS. We use the following transformation formula with calibration factor (CF). We substitute -83 for the CF (ALOS User Interface Gateway, 2009).

$$\mathrm{NRCS(dB)}=10\times\log_{10}(\mathrm{DN}^2)+\mathrm{CF} \qquad (1)$$

Next, the other orthoimage is generated from reflection intensity values taken from LiDAR point cloud data. In this procedure, the reflection intensity values are projected into DSM generated from LiDAR data, as shown in Figure 2 and Figure 3.
We selected several corresponding points, such as road intersections, rivers, and bridges, from each orthoimage. Moreover, the affine transformation is applied to the image registration between SAR and LiDAR data.

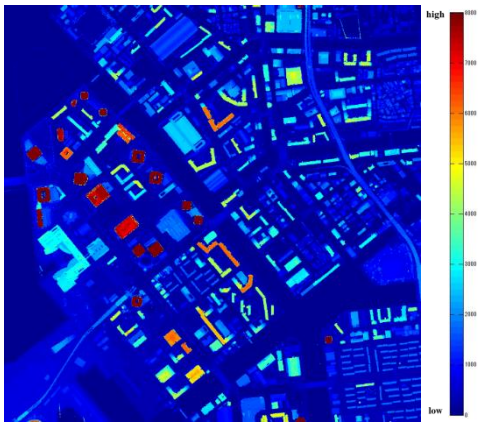

Figure 2. DSM

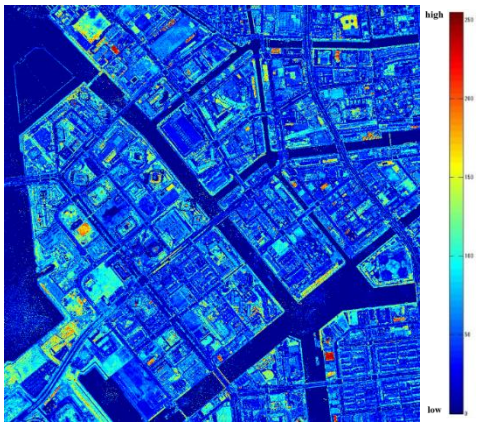

Figure 3. Reflection intensity orthoimage

2.2 Building footprint extraction

Building footprints are extracted from DSM, as shown in Figure 4.

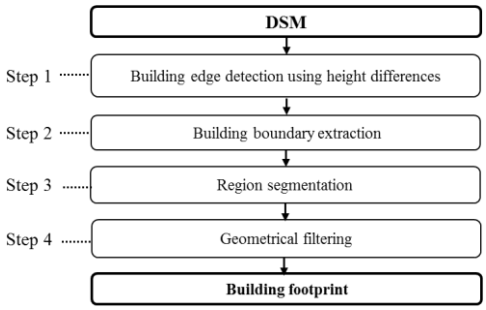

Figure 4. Process flow of building footprint extraction

Firstly, building edges are detected using height differences between building roofs and ground surfaces from DSM with a 3 × 3 operator. Although the building edges are discontinuous, approximate building features are detected in this step. Secondary, building boundaries are extracted. Discontinuous edges are connected to each other in the DSM with 8-neighborhood pixel filtering. The connected edges are defined as a building boundary. Thirdly, segmentation is applied to each region inside of the building boundary to refine building footprints. Although extracted region include many noises, such as bridges, street trees, and automobiles, an approximate geometry of each region is extracted in this step. Finally, the region segments are filtered with their perimeter and area to extract building footprints.

2.3 Building classification

In this study, three types of approaches are applied to our building classification. The first approach is to classify buildings (roof materials) with an average value of NRCS in each building footprint. Buildings are classified into several hierarchies with non-supervised classification using NRCS average value. The second approach is to classify buildings (roof materials) with reflection intensity values taken from LiDAR data. Buildings are also classified several hierarchies with non-supervised classification. The third approach is prepared to validate the above-mentioned approach. Height and area (3D data) taken from LiDAR data are used to estimate building types, such as a high-rise building, large facilities or house.

3. EXPERIMENT

In our experiment, we selected Toyosu and Monzennakacho town in Tokyo as our study area. This area includes various types of buildings, such as residential houses, high-rise buildings and shopping malls, as shown in Figure 5.

Building in each area

①	Residential area
②	Apartments
③	High-rise buildings
④	Large-scale facilities (shopping malls)
⑤	Other facilities, such as school and company

Figure 5. Study area

We prepared point cloud data acquired with an airborne LiDAR and geocoded satellite SAR data, as shown in Table 1 and Table 2. Moreover, threshold values were used in building extraction and classification, as shown in Table 3.

Table 1. Specification of LiDAR data

Sensor	Observer	Date	Spatial resolution	number of points
Airborne LiDAR	Kokusai Kogyo Co., Ltd	7, March, 2011	0.5m（DSM）	4000 × 4000
Airborne LiDAR	Aero Asahi Corporation	26, August , 2013	0.1m	5498730

Table 2. Specification of SAR data

Sensor	Observer	Date	Spatial resolution	Geocoded	Polarized wave
ALOS PALSAR	JAXA	20, March, 2009	12.5m	Map North	HV

Table 3. Threshold values

	Step 1	Step 2	Step 3	Step 4	High-rise buildings	Large scale facilities	Residential
Height	2 m	0.2 m	2 m	---	50 m	---	---
Area	---	---	---	62.5 m^2	---	6250 m^2	500 m^2
Perimeter	---	---	---	5000 m	---	---	---
Perimeter/area	---	---	---	0.3	---	---	---

4. RESULTS

We extracted 911 buildings from DSM. First, Figure 6 shows a result in the step 1. White edges indicate extracted building boundaries with height differences. Next, Figure 7 shows a result in the step 2. Dilated white edges are refined building boundaries. Figure 8 shows a result in the step 3. White regions indicate extracted building footprints. Figure 9 shows a result in the step 4.

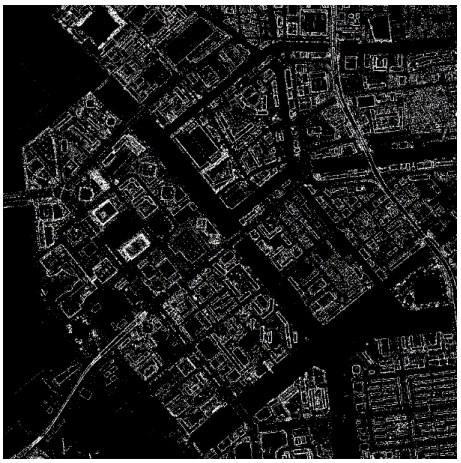

Figure 6. Result in the step 1

Figure 7. Result in the step 2

Figure 8. Result in the step 3

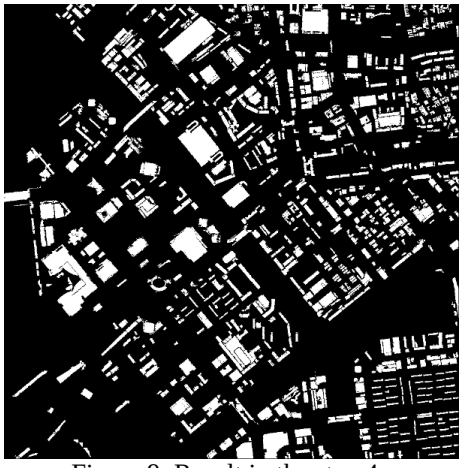

Figure 9. Result in the step 4

Classified buildings with NRCS are shown in Figure 10. NRCS values are indicated from blue (lower NRCS) to red (higher NRCS) color. Classified buildings with LiDAR reflection intensity are shown in Figure 11. LiDAR reflection intensity values are indicated from blue (lower intensity) to red (higher intensity) color.

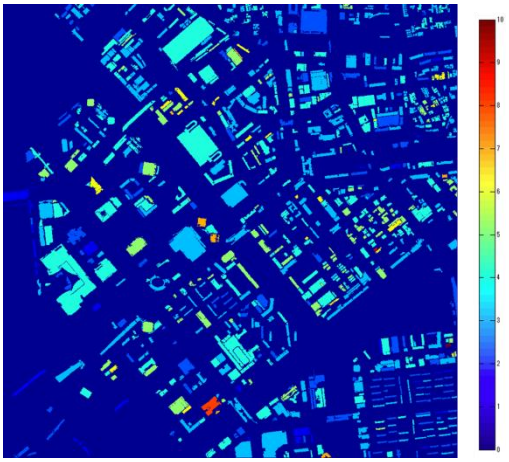

Figure 10. Classified buildings with NRCS

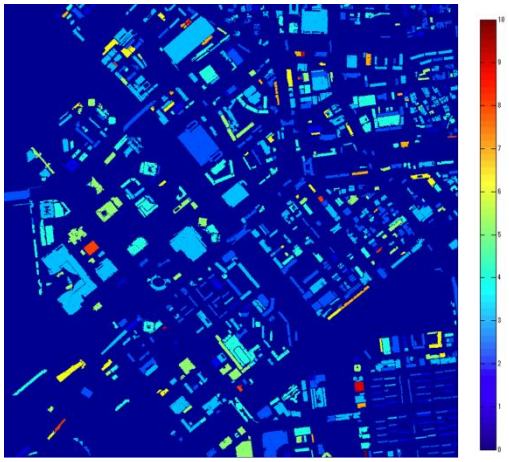

Figure 11. Classified buildings with LiDAR reflection intensity

Classified buildings with 3D data are shown in Figure 12. Color index indicates building attributes. We extracted three attributes, such as high-rise buildings (red), large-scale facilities (orange), and residential houses (green).

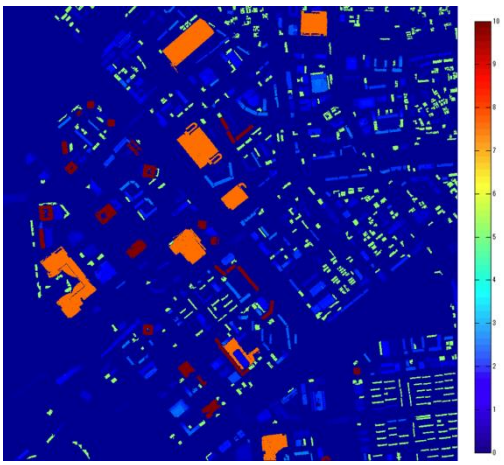

Figure 12. Classified buildings with 3D data

5. DISCUSSION

Classification results are summarized as shown in Table 4. This table shows the number of buildings which belongs to each cluster. In the classification with NRCS, we have confirmed that spatial resolution was too low to recognize small residential buildings and complex roofs of large buildings. In our experiment, supervised classification in the building extraction was affected by speckle noises. Therefore, we would propose speckle noise filtering before the classification.

Table 4. Classification results with NRCS

Cluster number	1	2	3	4	5	6	7	8	9	10
Classified buildings	30	161	322	266	100	22	7	1	1	1

Moreover, in our object extraction process, buildings were extracted from DSM in our object extraction process. Although visual checks were required to determine the best threshold values to extract buildings, several small noises including automobiles were left as unknown objects in the DSM. Semantics, such as road connections, might be one of approaches to improve our feature extraction accuracy. Moreover, although shadow detection is required, we can focus on a combination of LiDAR data with aerial images.

In the classification with LiDAR reflection intensity values, it was also difficult to classify small buildings, because spatial resolution and intensity feature quantity were insufficient to recognize building types.

On the other hand, high-rise buildings and large-scale facilities were classified successfully, because area and height were reliable data in the classification. As we can partly predict attribute from them, shape and scale might be index of first in the classification.

Although we focused on building roofs, we can focus on an opportunity to acquire more details of buildings with aerial LiDAR, as shown in Figure 13. Thus, we would improve our classification with estimations of wall surface and smaller object of buildings.

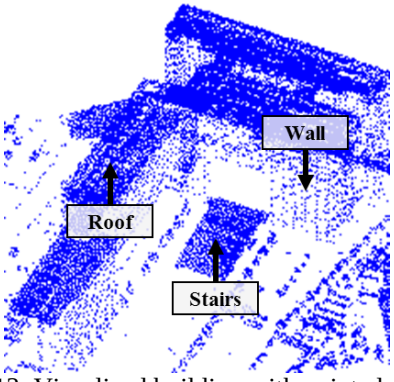

Figure 13. Visualized building with point cloud data

6. CONCLUSION

In this paper, we have focused on an integration of LiDAR with SAR data to achieve the frequent map update with attribute data acquisition. Firstly, we generated DSM from point cloud acquired with airborne LiDAR. Secondary, the DSM was registered the SAR data to overlay with NRCS calculated from the SAR data. Thirdly, buildings are extracted from the DSM. Finally, we classified buildings in the DSM into several clusters.
In our experiment, we prepared point cloud data acquired with an airborne LiDAR and satellite SAR data acquired with ALOS PALSAR in Tokyo. Next, we extracted 911 buildings from DSM. Although our result included noises such as bridges and automobiles, we classified buildings into 10 clusters with average NRCS values. In this study, we clarified that a combination of airborne LiDAR data and satellite SAR data can extract and classify buildings in urban area. In our future works, we will apply the supervised approach to improve our classification accuracy.

REFERENCES

[1] Antonarakis, A.S., Richards, K.S., Brasington, J., 2008. Object-based land cover classification using airborne LiDAR, Remote Sensing of Environment, Volume 112, Issue 6, pp.2988-2998.

[2] ALOS User Interface Gateway, 2009. PALSAR Calibration Factor Updated, Retrieved January 21, 2014, from http://www.eorc.jaxa.jp/en/about/distribution/info/alos/20090109en_3.html.

[3] Haala, N., Kada, M., 2010. An update on automatic 3D building reconstruction, ISPRS Journal of Photogrammetry and Remote Sensing Volume 65, Issue 6, pp.570-580.

[4] Japan Aerospace Exploration Agency, 2014. Advanced Observing Satellite-2 "DAICHI-2" (ALOS-2), Retrieved July 27, 2013, from http://global.jaxa.jp/projects/sat/alos2/.

[5] Sithole, G., Vosselman, G., 2003. Automatic structure detection in a point-cloud of an urban landscape, Remote Sensing and Data Fusion over Urban Areas. 2nd GRSS/ISPRS Joint Workshop on, pp.67-71.

[6] Tupin, F., Roux, M., 2003. Detection of building outlines based on the fusion of SAR and optical features, ISPRS Journal of Photogrammetry and Remote Sensing Volume 58, Issue 1–2, pp.71–82.

[7] Uchiyama, S., Inoue, H., Suzuki, H., 2014. Approaches for Reconstructing a Three-dimensional Model by SfM to Utilize and Apply this Model for Research on Natural Disasters, Volume 81, pp.37-60.

[8] Uemura, T., Uchimura, K., koutaki, G., 2011. Road Extraction in Urban Areas using Boundary Code segmentation for DSM and Aerial RGB images, Journal of The Institute of Image Electronics Engineers of Japan, Volume 40, No.1, pp.74-85.

[9] Zhang, K., Yan, J., Chen, S., 2006. Automatic construction of building footprints from airborne LIDAR data, IEEE Transactions on Geoscience and Remote Sensing, Volume 44, No. 9, pp.2523-2533.

ACKNOWLEDGMENT

This work is supported by Japan Aerospace Exploration Agency. Moreover, our experiments are supported by Kokusai Kogyo Co., Ltd and Aero Asahi Corporation.